Fast Hankel Transform Algorithms for Optical Beam Propagation

Timothy M. Pritchett

Army Research Laboratory

Adelphi, MD 20783-1197

Fast Hankel Transform Algorithms for Optical Beam Propagation

Timothy M. Pritchett
Sensors and Electron Devices Directorate

Abstract

Essential for the development of low-f-number eye and sensor protection systems is an accurate model for the propagation of a widely diverging laser beam through a nonlinear medium. This problem may be solved numerically with the well-known "split-step" procedure, in which the effects of propagation are computed separately from those arising from nonlinear absorption and refraction. For a cylindrically symmetric beam, the propagation phase of each step in the process is most conveniently calculated in the Hankel transform domain; each step thus requires numerical computation of a discrete Hankel transform followed by an inverse transform. Accordingly, we seek an algorithm for efficient numerical computation of the Hankel transform that preserves the transform's invertibility. This report summarizes the relevant properties of the Hankel transform and of the closely related Fourier transform, it reviews existing fast Hankel transform algorithms (proposing several modest improvements in one), and it evaluates those methods in terms of their suitability for the beam propagation application of interest.

Contents

Figures

1. Introduction

Applications of the Fourier-Bessel transform, commonly known as the Hankel transform, arise in a variety of fields, including signal processing, optics, acoustics, geophysics, and molecular biology. In optics, the Hankel transform appears in many contexts, not the least of which is the propagation of cylindrically symmetric laser beams. The wide utility of the Hankel transform has ensured a continuing interest in the development of efficient methods for its numerical computation, and a variety of "fast Hankel transform" algorithms has emerged over the past quarter-century [1–5]. This report aims to evaluate these methods in terms of their utility in calculations involving the propagation of optical beams.

This report is organized as follows. In the following section, we define the Hankel transform and inverse transform of a function. The Hankel transform is intimately related to its better known cousin, the Fourier transform, and in section 3, we remind the reader of several properties of the Fourier transform that will prove necessary in our later development. Section 4 of this report describes the particular application to optical beam propagation that motivates our interest in fast Hankel transform algorithms. Any numerical proccedure for computing a Hankel transform will necessarily involve a domain of integration that is only finite in extent, and section 5 examines the implications of this for the invertibility of the numerical transform. Section 6 reviews several methods for efficient numerical computation of Hankel transforms, and section 7 evaluates the most promising of these for use in our particular application.

2. Definition

The standard Hankel transform of order ℓ of a function $f(r)$ on the half-line $0 < r < \infty$ is defined as

$$g(\rho) = \mathcal{H}_\ell[f](\rho) = 2\pi \int_0^\infty r f(r) J_\ell(2\pi\rho\, r)\, d r\ ,\tag{1}$$

where $J_\ell(x)$ is the Bessel function of the first kind of order ℓ. The variable in the transform domain, ρ, may be thought of as a "spatial frequency," *i.e.*, the quantity $\kappa = 2\pi\rho$ is a wavenumber. The inverse transform is given by

$$f(r) = \mathcal{H}_\ell^{-1}[g](r) = 2\pi \int_0^\infty \rho g(\rho) J_\ell(2\pi\,\rho\, r) d\rho\ .\tag{2}$$

Hankel's integral formula [6] may be obtained from the above definitions by using (1) to substitute for $g(\rho)$ in (2). This important result is valid for any real $\ell \geq -1/2$ so long as (a) f and its first derivative are sectionally continuous on each bound interval, (b) $r^{1/2} f(r)$ is absolutely integrable from zero to infinity, and (c) f is defined as its mean value at each point of discontinuity. From Hankel's integral formula, we deduce the following "orthogonality relation" for Bessel functions on the half line:

$$\int_0^\infty u\, J_\ell(u\, v)\, J_\ell(u\, v')\, d u = \frac{\delta(v - v')}{v}\tag{3}$$

Equation (3) ensures the invertibility of the Hankel transform, *i.e.*, guarantees that the successive operations of Hankel transform followed by inverse Hankel transform reproduce the original input function.

3. A Word About Fourier Transforms

The Hankel transform is closely related to the two-dimensional (2-D) Fourier transform of a cylindrically symmetric function. Since the Fourier transform will itself play an important role in the particular application to optics that this report is intended to addresss, we pause here to briefly examine the Fourier transform and its relationship to the Hankel transform and to remind the reader of some properties of the Fourier transform that we will require.

3.1 Conventions

Several conventions are commonly used to define the Fourier transform; ours follow. Let $F(\vec{x})$ be a function, in general complex, on the n-dimensional real space R^n. We define the Fourier transform of $F(\vec{x})$, denoted $\mathcal{F}[G](\vec{\kappa})$, as

$$G(\vec{\kappa}) = \mathcal{F}[F](\vec{\kappa}) = \int_{-\infty}^{\infty} F(\vec{x})e^{i\,\vec{x}\cdot\vec{\kappa}}d^n x \tag{4}$$

and we define the inverse transform as

$$F(\vec{x}) = \mathcal{F}^{-1}[G](\vec{x}) = (2\pi)^{-n}\int_{-\infty}^{\infty} G(\vec{\kappa})e^{i\,\vec{x}\cdot\vec{\kappa}}d^n \kappa \ . \tag{5}$$

3.2 Relation Between Hankel and Fourier Transforms

In two dimensions, we may express the integral (4) in plane polar coordinates,

$$G(\kappa,\phi) = \int_0^{\infty}\int_0^{2\pi} rF(r,\theta)e^{\cos(\theta-\phi)\kappa r}d\,\theta d\,r \ ,$$

where $\kappa = [\kappa_x^2 + \kappa_y^2]^{1/2}$ is the wavenumber. At this point, we specialize to the case of a transforming function of the form $F(r,\theta) = f(r)e^{i\,m\,\theta}$, where m is an integer. Employing the identity

$$e^{i\,x\,\sin\theta} = \sum_{n=-\infty}^{\infty} J_n(x)e^{i\,n\,\theta} \ ,$$

we can in this case perform the integration over θ and so obtain

$$G(\kappa,\phi) = 2\pi i^m e^{im\phi}\int_0^{\infty} rf(r)J_m(\kappa\,r)d\,r \ .$$

Setting $\kappa = 2\pi\rho$, we see that the 2-D Fourier transform of $F(r,\theta) = f(r)e^{i\,m\,\theta}$ is related to the mth-order Hankel transform of the "radial function" $f(r)$ by

$$G(2\pi\rho,\phi) = \mathcal{F}[F](2\pi\rho,\phi) = i^m e^{i\,m\,\phi}\mathcal{H}_m[f](\rho) \ ,$$

3

where $\mathcal{H}_m[f](\rho)$ is the Hankel transform of f as defined in (1). In much the same way, one may start from the definition of the inverse Fourier transform (5) and show that in two dimensions the inverse transform of a function of the form $G(2\pi\rho, \phi) = g(\rho)e^{-im\phi}$ is given by

$$F(r, \theta) = 2\pi(-i)^m e^{-im\theta} \int_0^\infty \rho g(\rho) J_m(2\pi\rho r) \, d\rho \, ,$$

or, comparing the integral on the right-hand side with that in (2),

$$\mathcal{F}^{-1}[G](r, \theta) = (-i)^m e^{-im\theta} \mathcal{H}_m^{-1}[g](r),$$

where $\mathcal{H}_m^{-1}[g](r)$ is the mth-order inverse Hankel transform of $g(\rho)$.

In optics, we are primarily interested in the case $m = 0$, which corresponds to a cylindrically symmetric function $F(r)$. As we have just seen, such a function's Fourier transform in two dimensions is identical to its Hankel transform. Similarly, the inverse Fourier transform in two dimensions of a circularly symmetric $G(\kappa)$ is identical to the inverse Hankel transform.

3.3 The Correlation Theorem

The cross-correlation of two functions $\alpha(\vec{x})$ and $\beta(\vec{x})$ is defined by the integral

$$\mathrm{corr}[\alpha, \beta](\vec{x}) = \int_{-\infty}^\infty \alpha(\vec{x} + \vec{u}) \, \beta(\vec{u}) \, d^n u \, .$$

If we consider now the Fourier transform (4) of $\mathrm{corr}[\alpha, \beta]$,

$$\mathcal{F}[\mathrm{corr}[\alpha, \beta]](\vec{\kappa}) = \int_{-\infty}^\infty \int_{-\infty}^\infty \alpha(\vec{x} + \vec{u}) \, \beta(\vec{u}) \, e^{i\vec{x}\cdot\vec{\kappa}} d^n u \, d^n x \, ,$$

we can, simply by interchanging the order of the integrations and making a change of variable, prove the well-known correlation theorem:

$$\begin{aligned} \mathcal{F}[\mathrm{corr}[\alpha, \beta]](\vec{\kappa}) &= \int_{-\infty}^\infty \alpha(\vec{w})e^{i\vec{w}\cdot\vec{\kappa}} d^n w \int_{-\infty}^\infty \beta(\vec{u}) \, e^{-i\vec{u}\cdot\vec{\kappa}} d^n u \\ &= \mathcal{F}[\alpha](\vec{\kappa}) \, \mathcal{F}[\beta](-\vec{\kappa}) \, . \end{aligned}$$

This theorem, in combination with well-known fast Fourier transform (FFT) algorithms, will be applied to efficiently compute the sums that arise in a discrete analog of the Hankel transform.

4. The Hankel Transform in Optical Beam Propagation

Our interest in fast Hankel transform algorithms arises from the need to calculate the effects of laser beam propagation through a variety of media. Some of these materials exhibit an optical response that is linear even for beams of extremely high intensity, while others provide a response that is highly nonlinear. Frequently, the optical systems into which these media are incorporated are characterized by a low *f*-number. In such systems, the usual simplifying assumption of beam paraxiality is invalid. Choosing the *z*-axis parallel to the primary direction of propagation of the beam, one typically writes the electric field of a single-frequency component of the beam in terms of a spatial envelope $\psi(\vec{x}, z)$ thus: $E(\vec{x}, z, t) = \psi(\vec{x}, z) \exp[i(kz - \omega t)]$. In a low-*f*-number system, the spatial envelope $\psi(\vec{x}, z)$ satisfies the nonparaxial wave equation, which, in the case of a linear medium, reduces to the following form:

$$\left(\frac{\partial}{\partial z} - \frac{i}{2k} \frac{\partial^2}{\partial z^2} \right) \psi(\vec{x}, z) = \frac{i}{2k} \nabla_T{}^2 \psi(\vec{x}, z) . \tag{6}$$

Here, $\nabla_T{}^2$ is the transverse Laplacian.

$$\nabla_T{}^2 = \frac{\partial^2}{\partial x^2} + \frac{\partial^2}{\partial y^2} = \frac{\partial^2}{\partial r^2} + \frac{1}{r} \frac{\partial}{\partial r} + \frac{1}{r} \frac{\partial^2}{\partial \phi^2}$$

(In the paraxial approximation, one drops the term in (6) involving the second derivative with respect to *z*.)

The nonparaxial propagation operator,

$$P = \exp \left[\frac{iz \nabla_T{}^2}{k + \sqrt{k^2 + \nabla_T{}^2}} \right],$$

generates from the "initial value" $\psi(\vec{x}, z = 0)$ an exact solution to (6), $\psi(\vec{x}, z) = P\psi(\vec{x}, 0)$, as one may easily verify by direct substitution [7, 8]. In order to implement the operator P, it is convenient use (5) to write $\psi(\vec{x}, 0)$ in terms of its Fourier representation. Then

$$\psi(\vec{x}, z) = P\psi(\vec{x}, 0) = \frac{1}{(2\pi)^2} \int_{-\infty}^{\infty} \int_{-\infty}^{\infty} d^2\kappa \exp \left[\frac{-iz\kappa^2}{k + \sqrt{k^2 - \kappa^2}} \right] \mathcal{F}[\psi|_{z=0}](\vec{\kappa}) e^{-i\vec{\kappa} \cdot \vec{x}} , \tag{7}$$

where $\mathcal{F}[\psi|_{z=0}](\vec{\kappa})$ is the Fourier transform of $\psi(\vec{x}, 0)$ and $\kappa = [\kappa_x{}^2 + \kappa_y{}^2]^{1/2}$ is the transverse wavenumber. For a cylindrically symmetric beam, the envelope function's Fourier transform and its zero-order Hankel transform are identical: $\mathcal{F}[\psi|_{z=0}](\vec{\kappa}) = \mathcal{H}[\psi|_{z=0}](\kappa)$. (In order to make the notation less cumbersome, when no confusion can result, we frequently suppress the

subscript "*m*" in "$\mathcal{H}_m[\cdot]$" in the case of an order $m = 0$ transform.) Assuming a cylindrically symmetric beam, we write the integral over the κ-plane in polar coordinates and integrate over the angular variable, obtaining a Bessel function in the process. The result is

$$\psi(r, z) = \frac{1}{2\pi} \int_0^\infty d\kappa\, \kappa \exp\left[\frac{-iz\kappa^2}{k + \sqrt{k^2 - \kappa^2}}\right] \mathcal{H}[\psi|_{z=0}](\kappa) J_0(\kappa r) .$$

Noting that the above integral is simply the inverse Hankel transform of order zero and switching the variable in the transform domain from κ to ρ, we write this as

$$\psi(r, z) = \mathcal{H}^{-1}\left[\exp\left[\frac{-iz(2\pi\rho)^2}{k + \sqrt{k^2 - (2\pi\rho)^2}}\right] \mathcal{H}[\psi|_{z=0}]\right] . \tag{8}$$

Alternately, (8) may also be derived from the following representation for $\psi(\vec{x}, 0)$ in terms of zero-order Hankel transforms

$$\psi(r, 0) = \mathcal{H}^{-1}[\mathcal{H}[\psi|_{z=0}]](r) = 2\pi \int_0^\infty \rho \mathcal{H}[\psi|_{z=0}](\rho) J_0(2\pi\rho r) d\rho .$$

(This is none other than the Hankel integral formula, to which we alluded in sect. 2.) Now, with a transverse Laplacian reflecting the assumption of circular symmetry,

$$\nabla_T{}^2 J_0(2\pi\rho r) = \left(\frac{\partial^2}{\partial r^2} + \frac{1}{r}\frac{\partial}{\partial r}\right) J_0(2\pi\rho r) = -(2\pi\rho)^2 J_0(2\pi\rho r) ,$$

where the last equality follows from Bessel's equation of order zero. Thus,

$$P\psi(r, 0) = 2\pi \int_0^\infty \rho \mathcal{H}[\psi|_{z=0}](\rho) \exp\left[\frac{-iz(2\pi\rho)^2}{k + \sqrt{k^2 - (2\pi\rho)^2}}\right] J_0(2\pi\rho r) d\rho ,$$

and (8) follows.

The solution (8) is exact only for linear media. For the propagation of optical beams through nonlinear media, (8) is applied repeatedly for very small z in the split-step procedure introduced in optics by Feit and Fleck [9]. Each step involves a Hankel transform followed, after multiplication by the propagation operator P as represented in the ρ-domain, by an inverse transform. The solution generated by this procedure after a large number of propagation steps is reliable only to the extent that the numerical method used to compute the Hankel transform preserves the transform's invertibility. Put another way, if successive operations of Hankel transform followed by inverse transform fail to reproduce the original input function with reasonable accuracy, then any solution obtained from a multi-step procedure will after only a few steps have become so inaccurate as to be virtually useless.

Our particular application demands an approximate numerical procedure that will, to the greatest extent possible, preserve the invertibility of the Hankel transform; computational efficiency, while important, is a secondary concern.

5. The Effect of Finite Domains

In situations of physical interest, the function $f(r)$ may typically be taken to be non-vanishing only for r less than some maximum value b. Real optical systems are always characterized by an effective aperture of some sort, and even in the absence of an aperture, a function $f(r)$ arising in a physical problem will generally decrease sufficiently rapidly with distance that its effects at large r are negligibly small. Although it is less obvious, one may, in the same way, take the spatial frequency to have an upper bound, the maximum bandwidth β. The upper limit of integration in (1) is thus replaced by b, and in (2) by β. In such a case, it is convenient to introduce the dimensionless spatial variable $x = r/b$ and the dimensionless transform variable $y = \rho/\beta$ and to work with functions $f(x)$ and $g(y)$ defined on the unit interval. Defining $\gamma = b\beta$, the space-bandwidth product of the transformation, we rewrite the Hankel transform (1) as

$$g(y) = 2\pi\gamma\frac{b}{\beta} \int_0^1 xf(x)J_\ell(2\pi\gamma xy)dx \;, \tag{9}$$

and the inverse transform (2) as

$$f(x) = 2\pi\gamma\frac{\beta}{b} \int_0^1 yg(y)J_\ell(2\pi\gamma xy)dy \;. \tag{10}$$

We observe that, despite appearances, the ratio b/β is *not* dimensionless but carries units of length squared.

In order to assess the extent to which the imposition of cutoffs in the spatial and spatial frequency domains limits the invertibility of the transform, we turn now to some examples for which the Hankel transform may be computed analytically. In each case, we numerically compute the inverse transform integral (10) by Gaussian quadrature and compare the result to the original function.

5.1 "Top Hat" Input Function

Students of optics are familiar with the zero-order Hankel transform of the unit step function, $\Theta(b - r)$, which arises in the problem of Fresnel diffraction from a uniformly illuminated circular aperture of radius b. In this case, $f(x)$ is simply equal to unity and (9) can be performed analytically with the result:

$$g(y) = \frac{2\pi\gamma b}{\beta} \int_0^1 xJ_0(2\pi\gamma xy)dx = \frac{bJ_1(2\pi y\gamma)}{y\beta} \;. \tag{11}$$

We now numerically evaluate the inverse transform (10) using adaptive Gaussian quadrature with error estimation based on evaluation at Kronrod points; the numerical results are accurate to six decimal digits. Figure 1

Figure 1. Results of successive operations of Hankel transform followed by inverse Hankel transform on a unit "top hat" input.
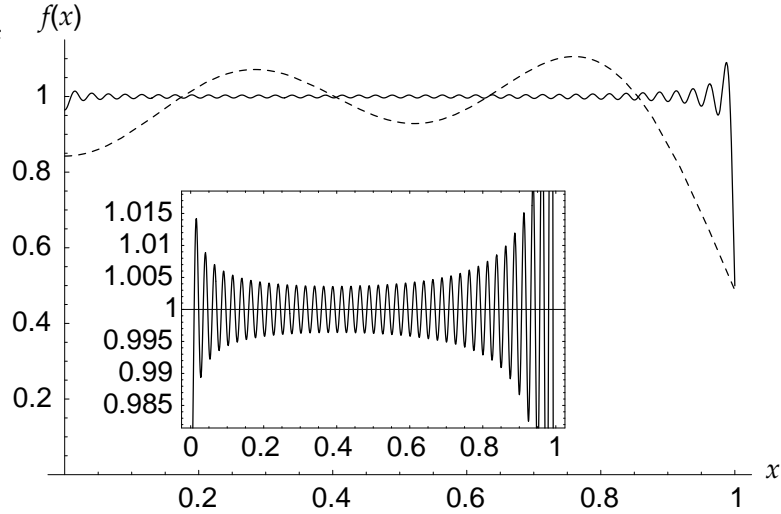
shows the result of performing this calculation for two different values of the space-bandwidth product: $\gamma = 2$ (dotted line) and $\gamma = 40$ (solid line); the insert depicts the results for $\gamma = 40$ on an expanded scale.

In the limit of infinite domains of integration in space and spatial frequency, the orthogonality relation (3) holds exactly, and application of the inverse transform (2) to the transformed function returns the original input function. For finite domains, we expect that the larger the space-bandwidth product, the more closely the result of the approximate transform or inverse transform will mirror the "true" result. In the present case, the transform (11) of the unit top hat function is exact, so the larger the cutoff β in spatial frequency (and thus the larger the space-bandwidth product γ) used in the approximate inverse transform, the more closely the twice-transformed function reproduces the original "top hat" input. The pair of curves in figure 1 graphically illustrates this.

At $x = 1$, where the input function is discontinuous, the integral converges to the mean value, $1/2$, as expected. Gibbs phenomena are observed in the vicinity of the discontinuity.

5.2   Uniform Annular Input Function

Similar to the top hat function discussed in the preceding section, the unit annular function that we consider here may be written as a sum of step functions: $\Theta(b/4 - r) - \Theta(3b/4 - r)$; it vanishes everywhere except on the open interval $(b/4, 3b/4)$, where it is equal to one. (At $r = b/4$ and $r = 3b/4$, where the function is discontinuous, it assumes the mean value of $1/2$.) The exact Hankel transform, performed analytically, is

$$g(y) = 2\pi\gamma\frac{b}{\beta}\int_{\frac{1}{4}}^{\frac{3}{4}} x J_0(2\pi\gamma xy)dx = \frac{b}{4y\beta}\left(3J_1\left(\frac{3\pi y\gamma}{2}\right) - J_1\left(\frac{\pi y\gamma}{2}\right)\right). \quad (12)$$

As before, the inverse transform (10) was evaluated numerically by adaptive Gaussian quadrature. Displayed in figure 2, the results for $\gamma = 2$ (line

8

Figure 2. Hankel transform followed by inverse Hankel transform of a unit annular input function.
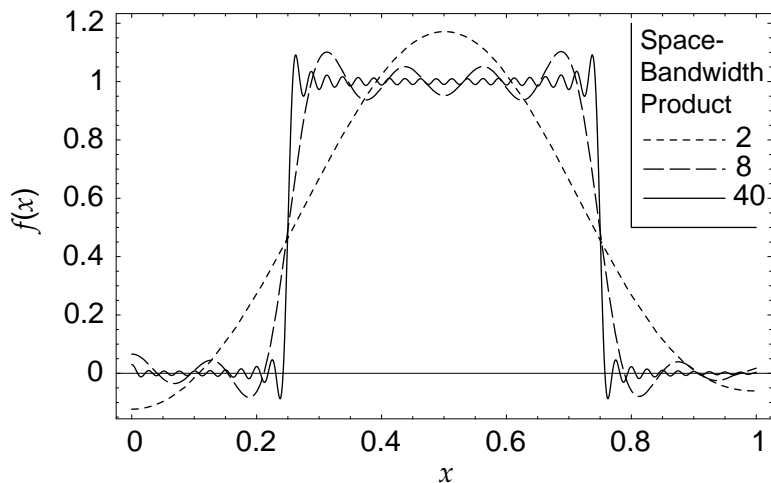
of short dashes), $\gamma = 8$ (line of long dashes), and $\gamma = 40$ (solid line) clearly illustrate how the accuracy of the approximate (finite) tranform (10) depends on the space-bandwidth product γ.

5.3 Parabolic Input Function

As a final example, we examine the parabolic input function $f(x) = x^2$, as is done in [5]. The fact that the upper limit of integration in the Hankel transform defined by (9) is 1, not infinity, effectively "clips" the input function to the unit interval; the effective input function used here is thus an "apertured parabola," equal to x^2 on the interval $0 \le x < 1$, vanishing for $x > 1$, and assuming the mean value of $1/2$ at the point of discontinuity, $x = 1$. Indeed, the "true" Hankel transform, equation (1), of the function $f(x) = x^2$, defined on the entire positive real axis, does not even exist, since the integral of x^3 from zero to infinity diverges! However, there is no such difficulty with the finite Hankel transform integral (9), which may be performed analytically, yielding

$$g(y) = \frac{2\pi\gamma b}{\beta} \int_0^1 x^3 J_0(2\pi\gamma xy)dx = \frac{b}{2y\beta}(J_1(2\pi y\gamma) - J_3(2\pi y\gamma)) . \qquad (13)$$

For completeness, we introduce $\eta = 2\pi\gamma y$ and use the well-known identities relating Bessel functions of adjacent orders [10] to rewrite (13) as

$$g(\eta) = \frac{2b\pi\gamma(2\eta J_0(\eta) + (\eta^2 - 4)J_1(\eta))}{\beta\eta^3} ,$$

analogous to equation (12) of reference [5].

Performing the inverse transform (10) numerically using the methods described before, we obtain the results shown in figure 3 for $\gamma = 2$ (line of short dashes), $\gamma = 8$ (line of longer dashes), and $\gamma = 40$ (solid line). These results reinforce the points made previously: namely, that the fidelity of the transform increases with the space-bandwidth product γ and that at points

9

Figure 3. Hankel transform followed by inverse Hankel transform of the parabola $f(x) = x^2$.
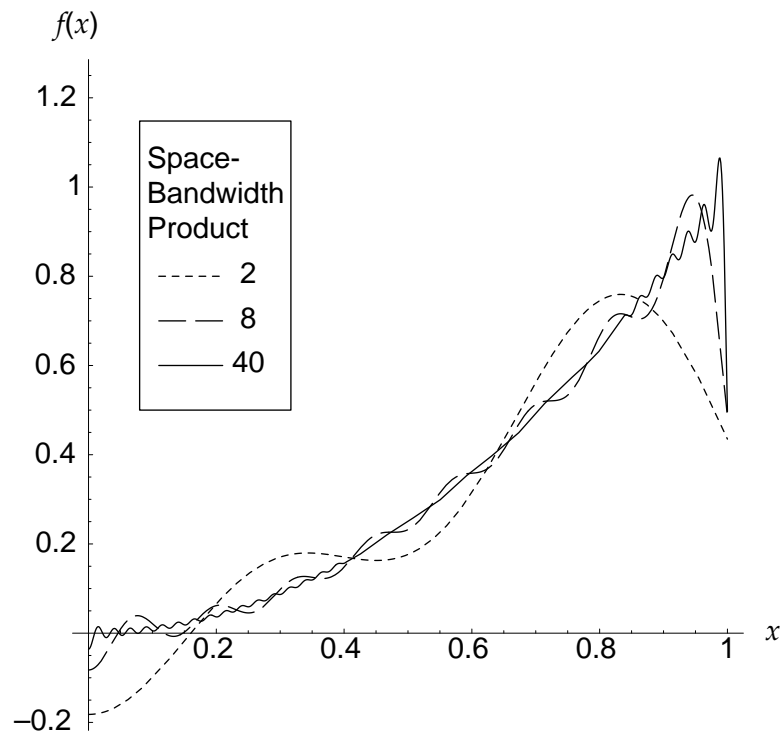
of discontinuity, the transform assumes the mean value of the function for every value of γ.

We turn now to a brief survey of various available methods for computing Hankel transforms numerically.

6.   Survey of Fast Numerical Methods

We wish to compute a numerical approximation to the Hankel transform integral (9) at a series of N spatial frequencies y_m, $m = 0, 1, \ldots N - 1$. The problem is immediately apparent: Naively sampling at N values $\{x_n\}$ of the normalized spatial variable and N normalized spatial frequencies $\{y_m\}$, $m, n = 0, 1, \ldots N - 1$, and then computing the integral (9) by a finite sum involves N^2 multiplications! Fortunately, we can do considerably better.

6.1   The "Quasi-Fast Hankel Transform"

Central to both the so-called "quasi-fast Hankel transform" methods described in this section and the "high-accuracy fast Hankel transform" of the following section (the names are due to Siegman [1] and Magni [5], respectively) is the exponential change of variables employed by Gardiner [11]:

$$r = r_0 e^{\alpha u}, \quad \rho = \rho_0 e^{\alpha v}. \tag{14}$$

With this change of variables, the Hankel transform integral (1) takes the form of a cross-correlation:

$$\hat{g}(v) = \int_{-\infty}^{\infty} \hat{f}(u) \, \hat{j}(u + v) du \;,$$

where $\hat{g}(v) = \rho_0 e^{\alpha v} g(\rho_0 e^{\alpha v})$, $\hat{f}(u) = r_0 e^{\alpha u} f(r_0 e^{\alpha u})$, and $\hat{j}(u + v) = 2\pi\alpha r_0 \rho_0 e^{\alpha(u+v)} J_\ell(2\pi r_0 \rho_0 e^{\alpha(u+v)})$. The correlation theorem, which we discussed in section 3.3, guarantees that a cross-correlation such as the one above is equal to the inverse Fourier transform of the product of the Fourier transforms of the functions in the correlation integral. Since discrete Fourier transforms can be computed with extremely high efficiency via the FFT methods that came into widespread use in the mid-1960s, the fact that one can recast the Hankel transform as a correlation is very fortuitous indeed.

The discrete Fourier transform of a function $f(u)$ is computed from a list of function values at evenly spaced values of u. Because the change of variable (14) between u and r is exponential, sampling at regular intervals in u implies geometric sampling in r, that is, in "real" space. While nonuniform sampling creates its own set of problems for certain applications, for our particular application to optics, it is actually something of an advantage. This happy state of affairs arises from the fact that the intensity of a laser beam is typically highest in the center of the beam and decreases as the distance r from the beam center increases. The geometric sampling in r leads to an increased density of grid points in the region of highest intensity, and since it is in this region that the optical properties of the medium would be expected to vary most rapidly with distance, it is precisely here that a finer grid is most desirable.

6.1.1 Original Formulation of Siegman

Among the earliest of the fast Hankel transform methods in current use is the "quasi-fast Hankel transform" introduced by Siegman [1]. Siegman chooses sampling points as a geometric series,

$$\rho_m = \rho_0 e^{\alpha m}, \quad r_n = r_0 e^{\alpha n}, \quad \text{for } m, \ n = 0, 1, \ldots N - 1 \,, \tag{15}$$

so that the resulting sum,

$$g(\rho_m) = \frac{2\pi\alpha}{\rho_m} \sum_{n=0}^{N-1} \phi_n \ j_{m+n} \,, \tag{16}$$

takes the form of a cross-correlation between discretely sampled functions:

$$
\begin{aligned}
\phi_n &= r_n f(r_n) \\
j_{m+n} &= \rho_m r_n J_\ell(2\pi\rho_m r_n) = \rho_0 r_0 e^{\alpha(m+n)} J_\ell(2\pi\rho_0 r_0 e^{\alpha(m+n)}) \,.
\end{aligned}
$$

If the number of sampling points N is chosen to be a power of 2, the discrete cross-correlation (16) may be computed very efficiently via a series of three $2N$-term fast Fourier transforms, each requiring only $2 N \log_2(2 N)$ multiplications. An end correction term suggested by Agrawal and Lax [12], $\pi r_0{}^2 f(r_0)$, may be added to (16) to account for the contribution to the Hankel transform integral from the excluded region $0 \le r < r_0$. The parameters α, r_0, and ρ_0 are arbitrary.

6.1.2 Improved Formulations by the Author

We have developed two related formulations of the quasi fast Hankel transform that apply specifically to the "windowed" Hankel transform (9) and of which the latter is modestly more accurate than Siegman's original formulation. We now describe these new formulations.

Approximation by "Right-hand Rectangles." We begin by defining sampling points as a geometric series on the unit interval $0 \le x, y \le 1$:

$$x_n = y_n = e^{\alpha(n-N)}, \quad n = 1, 2, \ldots N$$

This corresponds to taking $r_0 = be^{\alpha(1-N)}$ and $\rho_0 = \beta e^{\alpha(1-N)}$ in (15). The choice of identical sampling points in the spatial (x) and spatial frequency (y) domains is intended to facilitate inversion of the transform. The windowed Hankel transform integral (9) is then approximated by the sum

$$g(y_m) = 2\pi\gamma \frac{b}{\beta} \sum_{n=1}^{N} x_n f(x_n) J_\ell(2\pi\gamma x_n y_m)(x_n - x_{n-1}) \,, \tag{17}$$

in which

$$x_n - x_{n-1} = \begin{cases} x_1, & n = 1 \\ x_n(1 - e^{-\alpha}), & n = 2, 3, \ldots N \end{cases}$$

In effect, we are approximating the integrand in (9) by a series of rectangles, the height of each equal to the value of the integrand at the *right-hand edge* of the rectangle. One might expect that a better approximation to (9) could be obtained by choosing the height of each rectangle equal to the value of the integrand at the *center* of each rectangle, and this is indeed the case. We will develop an improved formulation based on "centered rectangles" in a moment. To conclude the present discussion, we observe that our choice of sampling points allows the sum in (17) to be evaluated as the cross-correlation

$$g(y_m) = 2\pi\gamma \frac{b}{\beta} \sum_{n=1}^{N} \phi_n j_{m+n} , \tag{18}$$

between the discretely sampled functions:

$$\phi_n = \begin{cases} x_1{}^2 f(x_1), & n = 1 \\ x_1{}^2 f(x_n)(1 - e^{-\alpha}), & n = 2, 3, \dots N \end{cases}$$

and

$$j_{m+n} = J_\ell(2\pi\gamma e^{\alpha(m+n-2N)}), \quad m, \ n = 1, 2, \dots N .$$

Approximation by "Centered Rectangles." In order to develop an improved formulation in the manner indicated previously, we define

$$\begin{aligned} \xi_0 &= 0 \\ \xi_n &= e^{\alpha(n-N)}, \quad n = 1, 2, \dots N, \end{aligned} \tag{19}$$

i.e., we take each ξ_n for $n \geq 1$ to be the same as the sampling point x_n used in the previous formulation. The points $\{\xi_n\}$, $n = 0, 1, \dots N$, divide the unit interval into N subintervals, the lengths of which are given above. We now select a new set of sampling points:

$$x_n = y_n = x_0 e^{\alpha n} , \quad \text{for } m, \ n = 0, 1, \dots N - 1, \tag{20}$$

and we choose the parameter x_0 so that, with the exception of the first, each of the sampling points lies at the center of its respective interval; this gives $x_0 = (e^\alpha - 1)e^{-\alpha N}/2$. The sum approximating the Hankel transform integral (9) is now given by

$$g(y_m) = 2\pi\gamma \frac{b}{\beta} \sum_{n=0}^{N-1} x_n f(x_n) J_\ell(2\pi\gamma x_n y_m)(\xi_{n+1} - \xi_n) .$$

This sum is a discrete cross-correlation of the same form as (18) but with the following functions.

$$\phi_n = \begin{cases} x_0 e^{-\alpha N} f(x_0), & n = 0 \\ x_0 e^{\alpha(2n-N)} f(x_n)(1 - e^{-\alpha}), & n = 1, 2, \dots N - 1 \end{cases}$$

$$j_{m+n} = J_\ell(2\pi\gamma x_0{}^2 e^{\alpha(m+n)}) , \quad m, \ n = 0, 1, \dots N - 1$$

13

After the cross-correlation sum is computed by FFT methods, one could, if desired, add an end correction term to the sum to reflect the fact that the first rectangle is not "centered."

$$\text{(correction)}_m = \frac{1}{2}e^{-2\alpha N}\{(e^{2\alpha}-1)f(x_0)J_\ell(2\pi\gamma x_0 y_m) + e^{2\alpha}f(\xi_1/2)J_\ell(2\pi\gamma\xi_1 y_m)\}$$

In both formulations, the parameter α is arbitrary. One should choose α so that the minimum grid spacing corresponds to the minimum separation in space (or spatial frequency) that one could resolve in an experimental measurement.

6.2 The "High-accuracy Fast Hankel Transform" of Magni et al.

Magni *et al.* [5] developed a method specifically for the evaluation of windowed Hankel transforms of order zero. This so-called "high-accuracy fast Hankel transform" bears many similarities to the "centered rectangle" formulation of the quasi-fast Hankel transform described in the preceding paragraphs. In both approaches, one divides the unit interval into the same N subintervals $\xi_n \leq x, y < \xi_{n+1}$, $n = 0, 1, \ldots N - 1$, with endpoints ξ_n defined in (19), and one chooses the same set of sampling points $\{x_n\}$ according to (20) so that there is exactly one point per subinterval and each point except the first lies at the midpoint of its subinterval. Where the two approaches differ is in the function that one approximates as a series of "centered rectangles," *i.e.*, the function that one takes to be a constant over each subinterval. In the quasi-fast Hankel transform, one approximates by rectangles the entire integrand of the windowed Hankel transform integral (9), whereas in the high-accuracy fast Hankel transform, one approximates only the input function f. In the latter approach, one proceeds by performing the integration over each subinterval analytically.

$$\frac{2\pi\gamma b}{\beta}\int_{\xi_n}^{\xi_{n+1}}f(x_n)J_0(2\pi\gamma yu)u\,du = \frac{bf(x_n)}{y\beta}(J_1(2\pi\gamma y\xi_{n+1})\xi_{n+1} - J_1(2\pi\gamma y\xi_n)\xi_n)$$

Summing this result over the N intervals, one obtains a discrete approximation to the Hankel transform (9):

$$g(y_m) = \frac{b}{\beta y_m}\sum_{n=0}^{N-1}(f(x_n) - f(x_{n+1}))\xi_{n+1}J_1(2\pi\gamma y_m\xi_{n+1})$$

where $f(x_N)$ is defined to be zero. Because the sampling points lie in geometric progression, this sum can be computed as the cross-correlation

$$g(y_m) = \frac{b}{\beta y_m}\sum_{n=0}^{N-1}\tilde{\phi}_n\tilde{j}_{m+n}$$

between the discretely sampled functions:

$$\widetilde{\phi}_n = \begin{cases} (f(x_0) - f(x_1))\, e^{\alpha(1-N)} \times \text{(end correction)}, & \text{for} \quad n = 0 \\ (f(x_n) - f(x_{n+1}))\, e^{\alpha(n+1-N)}, & \text{for} \quad n = 1, 2, \ldots N-1 \end{cases}$$

$$\widetilde{j}_{m+n} = J_1(2\pi\gamma x_0 e^{\alpha(m+n+1-N)})$$

The end correction factor in the expression for $\widetilde{\phi}_0$ is equal to $(2e^{\alpha} + e^{2\alpha})[1 + e^{\alpha}]^{-2}/(1 - e^{-2\alpha})$ and arises from the integral over the first subinterval.

As in the previous formulations, the parameter α is arbitrary. Magni *et al.* report that best results are obtained by choosing the value of α so as to make the first and last subintervals of equal width [5].

The attempt to further improve the accuracy of this approach by approximating the input function *f* not by a series of rectangles but by a series of trapezoids, *i.e.*, by approximating *f* on the interval $\xi_n, \leq x < \xi_{n+1}$ by

$$\hat{f}(x) = f(\xi_n) + \left(\frac{f(\xi_{n+1}) - f(\xi_n)}{\xi_{n+1} - \xi_n} \right)(x - \xi_n)$$

is frustrated by the complexity of the expression obtained upon integration.

6.3   Other Fast Hankel Transform Methods

Oppenheim, Frisk, and Martinez [2] propose a number of methods based on the "projection-slice theorem," from which it follows that the Hankel transform is equal to the one-dimensional Fourier transform of the projection $p(x)$ of a 2-D function onto the *x*-axis:

$$p(x) = \int_{-\infty}^{\infty} f(x, y)dy = \int_{x}^{\infty} \frac{f(r)}{\sqrt{r^2 - x^2}} d(r^2) \ .$$

Unfortunately, the inherent complexity of these methods, as well as the lengthy computations that they entail, make them less than satisfactory.

The hybrid approach of Candel [3] computes the Hankel transform via a pair of companion algorithms, one for the low-order components and the other for the remaining orders. The combination can be shown to converge to the true transform to within a specified error. Unfortunately, this approach is limited by the individual shortcomings of its component algorithms: the first is not particularly fast, and the second, relying on the approximate representation of the Bessel function by a truncated series expansion, is not particularly accurate.

The clever 2-D fast Hankel transform algorithm of Murphy and Gallagher [4] is based on the result discussed in section 3.2 that the Hankel transform is the 2-D Fourier transform of a circularly symmetrical function. The Murphy-Gallagher procedure is superior to Siegman's implementation of the quasi-fast Hankel transform for many applications, particularly those in which the input data are already in a 2-D form or when one requires a 2-D output format. For our purposes, however, it is redundant; if we

were willing to endure the increased storage requirements associated with solving our nonparaxial beam propagation problem on a 2-D grid, then we would simply employ the propagation operator in the form (7) and would use 2-D FFT methods throughout the process.

7.   Assessment of the High-Accuracy Fast Hankel Transform Algorithm

In this section, we evaluate the merits of the high-accuracy fast Hankel transform method just described by employing it to numerically compute the Hankel transforms and inverse transforms of a variety of functions, to include the "top hat" function examined in section 5.1. We abstain from a similar assessment of the quasi-fast Hankel transform methods of section 6.1, since Siegman's implementation of this algorithm was shown by Magni *et al.* to be generally inferior to the high-accuracy fast Hankel transform method [5].

7.1   "Top Hat" Input Function

The high-accuracy fast Hankel transform method gives the exact transform of a constant function, as is obvious from the description of section 6.2; the numerical transform of the top hat input $f(x) = 1$ is thus identical to the analytic result (11). Using the high-accuracy method to numerically transform the top hat input for a given value of the frequency-bandwidth product γ, and then to compute the inverse transform at the identical value of γ, one obtains the results shown in figure 4 for $\gamma = 10$ (dotted line) and $\gamma = 40$ (solid line). Both the transform and the inverse transform were performed with 256 sampling points. The reader may verify from the expanded scale insert that the curve for $\gamma = 10$ displays exacts ten maxima, while that for $\gamma = 40$ displays exactly 40 such "humps."

Figure 4. High-accuracy numerical Hankel transform followed by inverse Hankel transform on a unit "top hat" input.

17
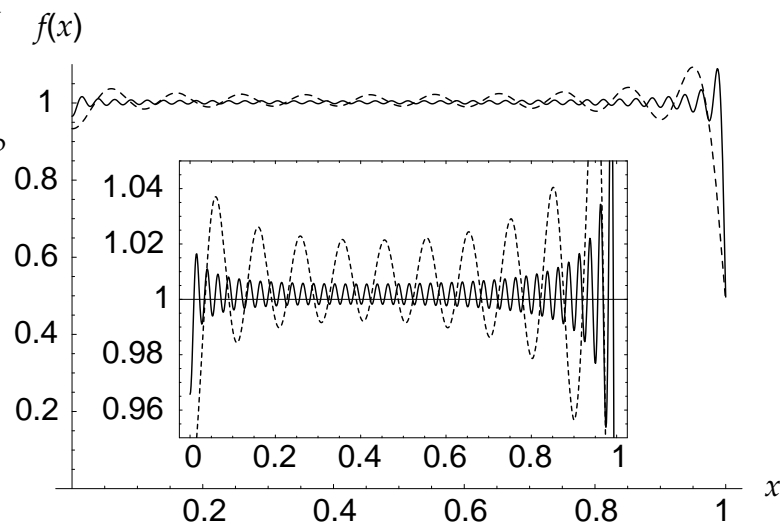
7.2   Parabolic Input Function

We conclude with an example of a function whose numerical high-accuracy fast Hankel transform is *not* exact; we consider the windowed Hankel transform of the parabolic input function $f(x) = x^2$ for space-bandwidth product $\gamma = 10$. The solid gray line in figure 5 depicts the analytic result (13), while the black dotted line shows the numerical results obtained with the high-accuracy fast Hankel transform with 256 sampling points.

In order to assess the degree to which the numerical procedure preserves the invertibility of the Hankel transform, we employ the high-accuracy fast Hankel transform method to numerically transform the parabolic input for a given value of γ and then to perform the inverse transform at the identical value of γ. Figure 6 illustrates the results of performing this sequence of operations with 256 sampling points for $\gamma = 4$ (dotted line), and with 1,048 sampling points for $\gamma = 40$ (solid line). The thick gray line shows the original input function.

These results, along with others not reported here, lead us to believe that the fast Hankel transform algorithm of [5] is more than adequate for the repetitive use required of it in a split-step beam propagation calculation.

Figure 5. Comparison of the analytic Hankel transform of $f(x) = x^2$ with the high-accuracy numerical transform.
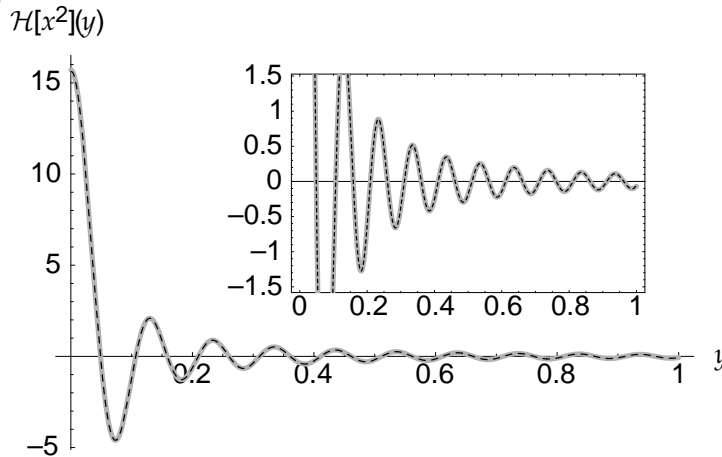
Figure 6. High-accuracy numerical Hankel transform followed by numerical inverse Hankel transform on a parabolic input .

18
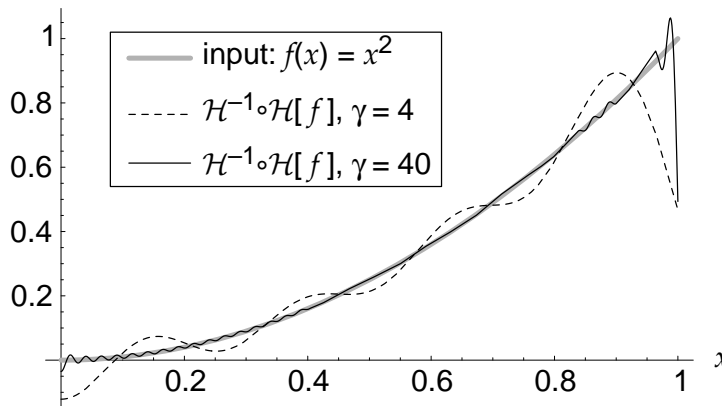
References

1. A. E. Siegman, "Quasi fast Hankel transform," Opt. Lett. **1**(1), 13–15 (1977).

2. Alan V. Oppenheim, George V. Frisk, and David R. Martinez, "Computation of the Hankel transform using projections," J. Acoust. Soc. Am. **68**(2), 523–529 (1980).

3. Sebastien M. Candel, "Dual algorithms for fast calculation of the Fourier-Bessel transform," IEEE Trans. **ASSP-29**(5), 963–972 (1981).

4. Patricia K. Murphy and Neal C. Gallagher, "Fast algorithm for the computation of the zero-order Hankel transform," J. Opt. Soc. Am. **73**(9), 1130–1137 (1983).

5. Vittorio Magni, Giulio Cerullo, and Sandro De Silvestri, "High accuracy fast Hankel transform for optical beam propagation," J. Opt. Soc. Am A **9**(11), 2031–2033 (1992).

6. Ruel V. Churchill, *Fourier Series and Boundary Value Problems, 2nd Ed.*, (McGraw-Hill: New York, 1969), p. 188.

7. M. D. Feit and J. A. Fleck, Jr., "Light propagation in graded-index optical fibers," Appl. Opt **17**(24), 3990–3998 (1978).

8. M. D. Feit and J. A. Fleck, Jr., "Beam nonparaxiality, filament formation, and beam breakup in the self-focusing of optical beams," J. Opt. Soc. Am. B **5**(3), 633–640 (1988).

9. M. D. Feit and J. A. Fleck, Jr., "Time-dependent propagation of hig energy laser beams through the atmosphere," Appl. Phys. **10**, 129–160 (1976).

10. See, for instance, J. D. Jackson, *Classical Electrodynamics, 2nd Ed.*, (Wiley: New York, 1975), p. 105.

11. D. G. Gardner, J. C. Gardner, G. Lausch, and W. W. Meinke, "Method for the analysis of multi-component exponential decays," J. Chem. Phys. **31**, 987 (1959).

12. G. P. Agrawal and M. Lax, "End correction in the quasi-fast Hankel transform for optical propagation problems," Opt. Lett **6**, 171–173 (1981).

Distribution

Admnstr
Defns Techl Info Ctr
ATTN DTIC-OCP
8725 John J Kingman Rd Ste 0944
FT Belvoir VA 22060-6218

DARPA
ATTN S Welby
3701 N Fairfax Dr
Arlington VA 22203-1714

Ofc of the Secy of Defns
ATTN ODDRE (R&AT)
The Pentagon
Washington DC 20301-3080

AMCOM MRDEC
ATTN AMSMI-RD W C McCorkle
Redstone Arsenal AL 35898-5240

US Army Rsrch Physics Div
ATTN AMXRO-PH D Skatrud
PO Box 12211
Research Triangle Park NC 27709-2211

US Army Rsrch Lab
ATTN AMSRL-RO-PP M Ciftan
PO Box 12211
Research Triangle Park NC 27709-2211

US Army TRADOC
Battle Lab Integration & Techl Dirctrt
ATTN ATCD-B
FT Monroe VA 23651-5850

CECOM NVESD
ATTN AMSEL-RD-NV-STD B Ahn
FT Belvoir VA 22060-5677

US Military Acdmy
Mathematical Sci Ctr of Excellence
ATTN MADN-MATH MAJ M Johnson
Thayer Hall
West Point NY 10996-1786

Natick Rsrch and Dev Ctr
ATTN SSCNC-IT M Nakashima
Natick MA 01760-5019

Dir for MANPRINT
Ofc of the Deputy Chief of Staff for Prsnnl
ATTN J Hiller
The Pentagon Rm 2C733
Washington DC 20301-0300

SMC/CZA
2435 Vela Way Ste 1613
El Segundo CA 90245-5500

TECOM
ATTN AMSTE-CL
Aberdeen Proving Ground MD 21005-5057

US Army ARDEC
ATTN AMSTA-AR-TD
Bldg 1
Picatinny Arsenal NJ 07806-5000

US Army Info Sys Engrg Cmnd
ATTN AMSEL-IE-TD F Jenia
FT Huachuca AZ 85613-5300

US Army Natick RDEC Acting Techl Dir
ATTN SBCN-T P Brandler
Natick MA 01760-5002

US Army Natick Rsrch & Dev Ctr
ATTN SSCNC-II B De Cristofano
Natick MA 01760-5019

US Army Simulation Train & Instrmntn
  Cmnd
ATTN AMSTI-CG M Macedonia
ATTN J Stahl
12350 Research Parkway
Orlando FL 32826-3726

US Army Tank-Automtv & Armaments Cmnd
ATTN AMSTA-TR-R-MS-263 R Goedert
Warren MI 48379-5000

US Army Tank-Automtv Cmnd RDEC
ATTN AMSTA-TR J Chapin
Warren MI 48397-5000

US Military Acdmy Dept of Physics
ATTN T Pritchett (10 copies)
West Point NY 10996

Nav Air Warfare Ctr
ATTN J Sheehy
48110 Shaw Rd Unit 5 Bldg 2187 Ste 1280
Patuxent River MD 20670-1906

Nav Rsrch Lab
ATTN Code 6336 G Mueller
4555 Overlook Ave SW
Washington DC 20375-5000

Nav Rsrch Lab
ATTN Code 5613 J Shirk
4555 Overlook Ave SW
Washington DC 20375-5345

Nav Surfc Warfare Ctr
ATTN Code B07 J Pennella
17320 Dahlgren Rd Bldg 1470 Rm 1101
Dahlgren VA 22448-5100

AFRL/MLPJ
ATTN S Guha
3005 P Stret Bldg 651 Ste 1
Wright-Patterson aFB OH 45433-7702

WL/MLPJ
ATTN C Ristich
3005 P Stret Ste 1 Bldg 651
Wright Patterson AFB OH 45433-7702

United States Military Academy
Dept of Elect Engrg & Computer Sci
Photonics Rsrch Ctr (10 copies)
West Point NY 10996

Hicks & Assoc Inc
ATTN G Singley III
1710 Goodrich Dr Ste 1300
McLean VA 22102

Palisades Inst for Rsrch Svc Inc
ATTN E Carr
1745 Jefferson Davis Hwy Ste 500
Arlington VA 22202-3402

Director
US Army Rsrch Lab
ATTN AMSRL-RO-D JCI Chang
ATTN AMSRL-RO-EN W D Bach
ATTN AMSRL-RO-P H Everitt
PO Box 12211
Research Triangle Park NC 27709

US Army Rsrch Lab
ATTN AMSRL-D D R Smith
ATTN AMSRL-DD J M Miller
ATTN AMSRL-CI-IS-R Mail & Records Mgmt
ATTN AMSRL-CI-IS-T Techl Pub (2 copies)
ATTN AMSRL-CI-OK-TL Techl Lib (2 copies)
ATTN AMSRL-SE J Pellegrino
ATTN AMSRL-SE-E H Pollehn (3 copies)
ATTN AMSRL-SE-E J Mait
ATTN AMSRL-SE-E W Clark
ATTN AMSRL-SE-EO A Mott (10 copies)
ATTN AMSRL-SE-EO G Wood (10 copies)
ATTN AMSRL-SE-EO J Goff
ATTN AMSRL-SE-EO M Ferry
ATTN AMSRL-SE-EO M Miller
Adelphi MD 20783-1197

REPORT DOCUMENTATION PAGE		*Form Approved* *OMB No. 0704-0188*

Public reporting burden for this collection of information is estimated to average 1 hour per response, including the time for reviewing instructions, searching existing data sources, gathering and maintaining the data needed, and completing and reviewing the collection of information. Send comments regarding this burden estimate or any other aspect of this collection of information, including suggestions for reducing this burden, to Washington Headquarters Services, Directorate for Information Operations and Reports, 1215 Jefferson Davis Highway, Suite 1204, Arlington, VA 22202-4302, and to the Office of Management and Budget, Paperwork Reduction Project (0704-0188), Washington, DC 20503.

1. AGENCY USE ONLY *(Leave blank)*	2. REPORT DATE December 2001	3. REPORT TYPE AND DATES COVERED Summary, Jan 2001 to Mar 2001

4. TITLE AND SUBTITLE Fast Hankel Transform Algorithms for Optical Beam Propagation	5. FUNDING NUMBERS DA PR: AH44 PE: 61102A
6. AUTHOR(S) Timothy M. Pritchett	

7. PERFORMING ORGANIZATION NAME(S) AND ADDRESS(ES) U.S. Army Research Laboratory Attn: AMSRL- SE-EO email: Tim Pritchett/arl@arl 2800 Powder Mill Road Adelphi, MD 20783-1197	8. PERFORMING ORGANIZATION REPORT NUMBER ARL-TR-2492
9. SPONSORING/MONITORING AGENCY NAME(S) AND ADDRESS(ES) U.S. Army Research Laboratory 2800 Powder Mill Road Adelphi, MD 20783-1197	10. SPONSORING/MONITORING AGENCY REPORT NUMBER

11. SUPPLEMENTARY NOTES
ARL PR: 1NE3AA
AMS code: 611102.H44

12a. DISTRIBUTION/AVAILABILITY STATEMENT Approved for public release; distribution unlimited.	12b. DISTRIBUTION CODE

13. ABSTRACT *(Maximum 200 words)*
Essential for the development of low-f-number eye and sensor protection systems is an accurate model for the propagation of a widely diverging laser beam through a nonlinear medium. This problem may be solved numerically with the well-known "split-step" procedure, in which the effects of propagation are computed separately from those arising from nonlinear absorption and refraction. For a cylindrically symmetric beam, the propagation phase of each step in the process is most conveniently calculated in the Hankel transform domain; each step thus requires numerical computation of a discrete Hankel transform followed by an inverse transform. Accordingly, we seek an algorithm for efficient numerical computation of the Hankel transform that preserves the transform's invertibility. This report summarizes the relevant properties of the Hankel transform and of the closely related Fourier transform, it reviews existing fast Hankel transform algorithms (proposing several modest improvements in one), and it evaluates those methods in terms of their suitability for the beam propagation application of interest.

14. SUBJECT TERMS Hankel transform, optical beam propagation, nonlinear optics			15. NUMBER OF PAGES 28
			16. PRICE CODE

17. SECURITY CLASSIFICATION OF REPORT Unclassified	18. SECURITY CLASSIFICATION OF THIS PAGE Unclassified	19. SECURITY CLASSIFICATION OF ABSTRACT Unclassified	20. LIMITATION OF ABSTRACT UL

NSN 7540-01-280-5500

Standard Form 298 (Rev. 2-89)
Prescribed by ANSI Std. Z39-18
298-102